Original Article

MicrostructuredChitosan/Poly(γ-glutamic acid)Polyelectrolyte Complex Hydrogels by Computer-aided Wet-spinning for Biomedical 3D Scaffolds.

Dario Puppi[1], Chiara Migone[1], Andrea Morelli[1], Cristina Bartoli[1], Matteo Gazzarri[1], Dario Pasini[2], Federica Chiellini[1*]

[1]BIOLab Research Group, UdR-INSTM Pisa, Department of Chemistry and Industrial Chemistry, University of Pisa, Italy

[2]Department of Chemistry and INSTM Research Unit, University of Pavia, via Taramelli 10, 27100, Pavia, Italy

Corresponding author: Federica Chiellini, Department of Chemistry and Industrial Chemistry, University of Pisa, Via Moruzzi 13, 56124, Pisa, Italy.

Email address: federica.chiellini@unipi.it

Tel: +39-050-2219333

Abstract

The application of Additive Manufacturing principles to hydrogel processing represents a powerful route to develop porous three-dimensional (3D) constructs with a variety of potential biomedical applications, such as scaffolds for tissue engineering and 3D *in vitro* tissue models. The aim of this study was to develop novel porous hydrogels based on amicrostructured polyelectrolyte complex (mPEC) between chitosan (CS) and

poly(γ-glutamic acid)(γ-PGA) by applying a computer-aided wet-spinning (CAWS) technique. The developed fabrication process was used to build up 3D porous hydrogels by collecting microstructured layers made of CS/γ-PGA one on top of the other.mPEC hydrogels were characterized and compared to CS/γ-PGA porous hydrogels with similar composition prepared by conventional freeze-drying technique. FT-IR analysis confirmed the formation of an electrostatic interaction between the two processed polymers in all the developed CS/γ-PGA hydrogels. The composition of the porous constructs as well as the employed processing techniques had a significant influence on the resulting swelling, thermal and mechanical properties. In particular, the combination of the ionic interaction between CS/γ-PGA and the defined internal microarchitecture of mPEC hydrogels provided a significant improvement of the compressive mechanical properties. Preliminary *in vitro* biological investigations revealed that mPEC hydrogels were suitable for the adhesion and proliferation of Balb/3T3 clone A31 mouse embryo fibroblasts. The encouraging results in terms of cytocompatibility and stability of the microstructure in aqueous solutions due to the ionic crosslinking suggest the investigation of the developed mPEC hydrogels as suitable scaffolds for 3D cells culture.

Keywords

Chitosan, poly (γ-glutamic acid), polyelectrolyte complexes, hydrogels, wet-spinning, additive manufacturing, 3D scaffolds.

Introduction

A great variety of polymers obtained from natural resources have been investigated for biomedical applications due to their inherent bioactivity given by chemical structure similarity with biopolymers constituting living organisms [1, 2]. The great interest for natural polymers stems from their renewability, biocompatibility and biodegradability combined with the presence of functional groups in their structural units that can confer a variety of biofunctionalities, such as biological signaling, cell adhesion, cell responsive degradation and re-modeling.

Polysaccharides are a class of natural polymers that have been widely proposed as scaffolding materials in tissue engineering applications as well as carriers for drug delivery systems [2, 3]. They can be obtained from different sources (microbial, animal and vegetable origin) and have generally low costs in comparison with other naturally-derived polymers, such as collagen. Chitosan (CS) is a cationic polysaccharide obtained by deacetylation of chitin, the second most abundant polysaccharide in nature, found in the exoskeleton of crustaceans, insects, and some fungi [4]. CS has been shown to possess many inherent advantages for biomedical applications including antibacterial activity, hydrophilic surface promoting cell adhesion, and good biocompatibility with acceptable host response and minimal foreign body reaction when implanted [5, 6]. It has been proved to be osteoconductive, enhancing bone formation both *in vitro* and *in vivo*[7, 8] and, given its structural similarity with various glycoaminoglycans, has been largely proposed as a

scaffolding material for cartilage tissue engineering [9].

CS hydrogels can be obtained through the formation of inter-chain physical interactions strong enough to form semi-permanent junction points in the molecular network, by means of non-covalent strategies that take advantage of electrostatic, hydrophobic and hydrogen bonding forces [10]. Polyelectrolyte complex(PEC) networks are formed by ionic interactions between the cationic CS chain and negatively charged polyelectrolytes without the use of organic precursors, catalysts, or reactive agents [10]. The complexation of CS with many different polyanions from natural resources (e.g. alginate, carrageenan, carboxymethyl cellulose, chondroitin sulphate, hyaluronic acid) or synthetic origin (e.g. poly(acrylic acid) and polyphosphoric acid) has been widely investigated [11].

Poly(γ-glutamic acid) (γ-PGA) is an anionic polypeptide made of D- and L-glutamic acid units that are connected by amide linkages between the α-amino and γ-carboxylic groups[12]. Produced predominantly by bacteria belonging to *Bacillus sp.* (e.g. *B.licheniformis* and *B. subtilis*) as an extracellular product of fermentation, γ-PGA is the major component of the viscous sticky mucilage in natto, a Japanese health food obtained from fermentation of soybeans. Due to its biodegradability and non-toxicity towards human and environment, γ-PGA has attracted great interest for different biomedical applications, including surgical adhesives, drug release and tissue engineering [13].Genetic engineering approaches capable to boost biopolymer production yields on *B. subtilis* laboratory strains have been demonstrated,[14]and the chemical

derivatization ofγ-PGA give access to processable biomaterials[15].

Few studies have proposed in the past years the ionic complexation of CS and γ-PGA as a means to provide the required physical-chemical, mechanical and bioactivity properties for the design of biomaterials tailored for specific biomedical applications. A recent article by Tsao *et al*. [16]reported on the development of γ-PGA/CS PEC hydrogels by freeze-drying with various molar ratios of amine to carboxylic acid groups. The developed porous hydrogels exhibited antibacterial activity and were effective in supporting Balb/3T3 fibroblasts adhesion and proliferation *in vitro*. *In vivo* studies showed the good potential of these PEC hydrogels for applications in wound dressing [17, 18] and bone regeneration [19].In addition, a CS/γ-PGA/carboxy-methyl-cellulose formulation was recently developed as injectable PEC scaffold for bone tissue engineering [20]. The optimized formulation showed short gelation time after injection and the resulting hydrogel well supported osteoblasts in-growth both *in vitro* and *in vivo*.

The application of Additive Manufacturing (AM) principles to process gel-forming materials has been extensively investigated in the last decade to design and fabricate fully-interconnected porous hydrogels for biomedical applications[21, 22]. AM techniques allow to build up three-dimensional (3D) structures with a computer-control layer-by-layer process through sequential delivery of energy and/or materials. A variety of AM approaches based on different working principles, that can be classified into laser-based,

nozzle-based and printer-based systems[21], have been developed to fabricate chemically- or physically-crosslinked hydrogels with pre-determined dimensions and porosity for different biomedical purposes, such as scaffolds for tissue engineering[23] cell encapsulation carriers[24] and matrices endowed with spatial and temporal release of growth factors to enhance therapeutic angiogenesis [25].

The aim of this study was the development of 3D porous PEC hydrogels based on CS and γ-PGA by means of a computer-aided wet-spinning (CAWS) technique based on AM principles that was recently applied to fabricate predesigned polymeric layered structures made of different biodegradable polyesters [26-29]. The experimental process to fabricate microstructured PEC (mPEC) hydrogels was optimized by investigating the effect of various processing parameters, such as polymeric solution composition, needle translation velocity and solution feed rate. The developed mPEC hydrogels were characterized for their physical-chemical, morphological, thermal, mechanical and swelling properties in comparison to analogous CS/γ-PGA hydrogels prepared by freeze-drying. Preliminary biological investigations were carried out in order to evaluate the ability of the prepared hydrogels to support cell adhesion and proliferation.

Materials and Methods

Materials

Chitosan (CS, medium molecular weight, Mw 108 kDa, deacetylation degree ~ 92%)[30], sodium tripolyphosphate (TPP), acetic acid and ethanol were purchased from Sigma-

Aldrich(Milan, Italy).Poly(γ-glutamic acid) (γ-PGA, 100kDa) was obtained from Natto Bioscience(Osaka, Japan). Phosphate buffered saline 0.1M (PBS 10X) was prepared by dissolving 2.0 g of KCl, 2.0 g of $KH_2PO_4 \bullet H_2O$, 80 g of NaCl, and 15.6 g of $Na_2HPO_4 \bullet 12H_2O$ in 1 liter of distilled water. The pH was adjusted to 7.4 with 10 N NaOH. The resulting PBS 10X was diluted ten fold with distilled water (PBS 1X, 0.01 M) and steam sterilized (121°C for 20 minutes) before used. All reagents used were commercially available (Carlo Erba, Milan, Italy).

Mouse embryo fibroblasts Balb/3T3 clone A31 cell line (CCL-163) was purchased from American TypeCulture Collection (ATCC). Dulbecco's modified Eagle's medium (DMEM), Dulbecco's Phosphate Buffer Saline (DPBS), calf serum, glutaraldehyde, sodium cacodylate, tetramethylsilane, Triton X-100,bovine serum albumin (BSA) were purchased from Sigma-Aldrich (Milan, Italy). L-glutamine and penicillin/streptomycin solution were obtained from Lonza (Portsmouth,USA). AlamarBlue®, Sytox®Green, phalloidin-tetramethylrhodamine B isothiocyanate(phalloidin-TRITC) and LIVE/DEAD® cell viability assay were purchased from Invitrogen (Milan, Italy). Plasmocin™ Treatment was purchased from InvivoGen (San Diego, USA).

3D Hydrogels fabrication

CS solutions were prepared by dissolving the polymer (4% w/v) in a0.2 M acetic acid aqueous solution under stirring for 16 h at room temperature. CS/γ-PGA mixtures were prepared following a procedure developed by Hsies *et al.* [31]. Briefly, γ-PGA was

dissolved in dH_2O under stirring for 1 h at room temperature. The desired amount of CS was then added to the γ-PGA solution (4% w/v total concentration of the polymeric phase in the mixture) and the suspension was left under vigorous stirring for 2 h. Acetic acid (1%v/v) was finally added and the obtained mixture was left under constant overnight stirring.

As reported in Table 1, a set of porous hydrogels were prepared by employing different process techniques, i.e. freeze-drying and computer-aided wet-spinning (CAWS), polymeric solutions with different composition, and different post-processing treatments.

Table 1. 3D hydrogels prepared by freeze-drying and CAWS.

Hydrogel Sample Nomenclature	**Processing Technique**	**CS/γ-PGA weight ratio in the mixture**	**Post-processing treatment**
CS-100	Freeze drying (frozen at -20 °C; lyophilized at -50 °C, 0.04 Torr)	100:0	TPP crosslinking
PEC-80:20		80:20	---
PEC-70:30		70:30	---
mCS-100	CAWS (Layered manufacturing through extrusion	100:0	TPP crosslinking
mPEC-80:20-PBS		80:20	Washing with EtOH/PBS mixtures

mPEC-80:20-TPP	directly into an ethanol bath)	80:20	TPP crosslinking

For the preparation of hydrogels by freeze-drying,2 ml of the polymeric mixture were poured into each well of a 12 well tissue culture plate, frozen at -20 °C for 24 h and then lyophilized at -50 °C and 0.04 Torr for 72 h.

Microstructured hydrogels were prepared by CAWS using an apparatus previously described[27]. In brief,10 ml of the polymeric solution were loaded into a syringe fitted with a blunt tip stainless steel needle (gauge 22)that was placed into a syringe pump (NE-100, New Pump Systems, Wantagh, NY, USA). The solution was forced through the needle at a controlled flow rate into an ethanol coagulation bath. The synchronized motion of the needle and of the coagulation bath controlled the deposition of the extruded solution mixture with a predefined 0-90° lay-down pattern to build up 3D hydrogel structures with a layer-by-layer process. Microstructured hydrogels were fabricated by employing an X-Y inter-fiber needle translation distance (d_{xy}) of 4 mm, and 2 mm staggered fiber spacing between successive layers with the same fiber orientation. The optimized initial distance between the tip of the needle and the bottom of the beaker was 4 mm and the interlayer needle translation was 200 µm.Microstructured CS (mCS-100) hydrogels were obtained by applying a solution

feed rate (F) of 1,5 mL/h and a deposition velocity (V_{dep}) of 100 mm/min, while microstructured CS/γ-PGAPEC (mPEC) hydrogels by applying F = 6,5 ml/h and V_{dep} = 600 mm/min.

The manufactured samples were left in the wet-spinning coagulation bathfor 24 h. mCS 100 hydrogels were extensively washed with a TPP solution (4% w/v) and left in the crosslinker solution overnight. mPEC hydrogels were treated following two different procedures: i)mPEC-80:20-PBS hydrogelswere extensively washed using a gradient series of ethanol/phosphate buffered saline (PBS 1X, pH 7.4) mixtures (90/10, 70/30, 50/50, 30/70 and 10/90 v/v) and then kept overnight in PBS; ii) mPEC-80:20-TPP hydrogels were extensively washed with a TPP crosslinker solution (4%w/v) and left in TPP overnight. Samples for physical-chemical characterization were rinsed four times in deionized water and then kept in deionized water overnight. After removal of excessive water on surface, scaffolds were frozen at -20 °C for 48 h and then lyophilized.

Films made of a blend between CS and γ-PGA for DSC analysis, were prepared in triplicate by solvent casting of a 4% w/v mixture (80:20 CS/γ-PGA weight ratio). For the preparation of the films, 4 ml of the solution were placed in a 3.5 cm diameter Petri plate and left for 48 h in a vacuum oven at 80°C and 0.1 bar.

Morphological characterization

Morphological investigation of top surface and cross-section(obtained by fracture in

liquid nitrogen) of the hydrogelsin the dry state was carried out by scanning electron microscopy (SEM, model JEOL JSM 300, Tokyo, Japan).

Determination of swelling degree

Swelling study was carried out at 37°C in either PBS 1X or DMEM. At specific time intervals, the samples were weighted after wiping the surface with a filter paper to remove excess swelling media. Three samples were tested for each typeof hydrogel. The swelling degree (SD) was calculated as:

$SD = [(W_s-W_d)/W_d] \times 100$

where W_d is the weight of the dry sample and W_s is the weight of the swollen sample.

Fourier transform infrared (FT-IR) spectroscopy measurement

FT-IR spectra were recorded as KBr pellets (1/20 mg) in the range of 4000-500 cm^{-1} by using a FT-IR spectrometer (FT/IR-410, Jasco Europe, Italy) with a resolution of 4 cm^{-1}. Each spectrum was recorded after 16 scans.

Thermal characterization

Thermogravimetric analysis (TGA) was performed using a TGA Q500 instrument (TA Instruments-Waters Division, Milan, Italy) in the temperature range 0-800 °C, at a heating rate of 10 °C/min and under a nitrogen flow of 60 ml/min. Differential scanning calorimetry (DSC) was performed under an 80 ml/min nitrogen flow rate by using a Mettler DSC-822 (Mettler Toledo, Italy). The samples were heated from 20 to 200°C,

cooled to 20 °C and finally heated to 200 °C at a heating and cooling rate of 10 °C/min. Glass transition temperature (T_g) was evaluated by considering the inflection point in the second cycle thermograms.

.

Mechanical characterization

The samples were cut into regular discs (diameter of 11 mm, thickness of 4 mm) and incubated in PBS 1X at 37 °C for 4 h. A uniaxial testing machine (DMTA V, Rheometric Scientific Inc., NJ, USA) equipped with parallel plates was employed to test the samples into a chamber filled with PBS 1X. The compressive properties of the hydrogels were assessed at a constant strain rate of 1 mm/min up to 80% strain. The tested samples were incubated in PBS 1X at 37°C for 2 h and the compressive analysis was then repeated. Low-strain and high strain modulus were defined as the slope of the two linear regions in the stress-strain curves. Five samples were tested for each typeof hydrogel.

Biological characterization

Hydrogels sterilization. Both types of hydrogels were exposed to ultraviolet (UV) light for 1 hour on each side and disinfected with 70% ethanol/water solution overnight. Samples were extensively washed with Dulbecco's phosphate buffered saline (DPBS) containing a penicillin/streptomycin solution (1%) and incubated with complete

medium before seeding.

Cell culture and cell seeding.Mouse embryo fibroblasts Balb/3T3 clone A31 were cultured in DMEM, supplemented with L-glutamine (4mM), penicillin:streptomycin solution (100 U/ml:100 μg/ml), calf serum (10%) and antimycotic agent. Cells were seeded at an appropriate density ($2x10^4$ cells/well) onto the hydrogels and cultured for 14 days at 37°C, 5% CO2. Cells cultured on tissue culture polystyrene (TCPS) were used as control.

Cell viability and cell proliferation. Quantitative evaluation of cell viability and proliferation was carried out by using the alamarBlue® assay on days 2, 5, 8 and 14 of culture, as previously described [32]. Briefly, the assay was performed by incubating cells-seeded hydrogels with the reagent for 24 hours. Measurements of resorufin dye absorbance were detected at 565 nm. The in vitro biological tests were performed in triplicates. Cell viability was further assessed by the LIVE/DEAD® assay at day 14 of culture. Samples were incubated with LIVE/DEAD®stain at a concentration of 2 μM calcein-AM and 4 μM ethidium homodimer-1 for 30 minutes. The presence of live (green) and non viable/dead (red) cells was assessed using a Nikon Eclipse TE2000 inverted microscope equipped with an EZ-C1 confocal laser (Nikon, Japan).

Scanning electron microscopy. Morphological analysis of Balb/3T3 cell line cultured on hydrogels was carried out by scanning electron microscopy (SEM) at day 14 of culture. After culture medium removal, each cell-seeded hydrogel was rinsed twice with

DPBS, and the cells were fixed with 2% glutaraldehyde solution in PBS 1X. After 1 hour of incubation, cells seeded constructs were rinsed again with PBS 1X and treated with sodium cacodylate 0.1 M pH 7.4 for approximately 1 minute. After cell fixation, specimens were dehydrated in ethanol solution of varying concentration (i.e. 10, 30, 50, 70, 90, and 100%, respectively) for 15 minutes at each concentration. Samples were dried in tetramethylsilane to remove any water traces. The fixed hydrogels were mounted on a SEM stub, coated with gold at 15 mA for 20 min, and observed by SEM at different magnifications (400-3000X).

Confocal Laser Scanning Microscopy (CLSM). Morphology of Balb/3T3 clone A31 cells cultured on hydrogels was investigated by means of confocal laser scanning microscopy (CLSM) at day 14 after seeding. Cells were fixed with 3.8% paraformaldehyde for 1 hour in PBS 1X at room temperature and permeabilized with a PBS 1X/Triton X-100 solution (0.2%) for 10 min. After blocking with 1%(w/v) BSA in PBS 1X for 30 min, cells were incubated with a PBS 1X solution of Sytox®green and phalloidin-TRICTfor 1 hour. Following incubation in the dye solution, samples were extensively washed with PBS 1X and observed using confocal microscopy. A Nikon Eclipse TE2000 inverted microscope equipped with EZ-C1 confocal laser (Nikon, Japan) and Differential Interference Contrast (DIC) apparatus were used to analyze the samples. An Argon Ion Laser (488 nm emission) and a solid-state laser (561 nm emission) were used to excite Sytox®green and TRICT fluorophore, respectively.

Images were captured with Nikon EZ-C1 software with identical settings for each sample and further merged with Nikon ACT-2U Software.

Statistical analysis

The data are represented as mean ± standard deviation. Statistical differences were analyzed using one-way analysis of variance (ANOVA), and a Tukey test was used for post hoc analysis. A p value < 0.05 was considered statistically significant.

Results and Discussion

Techniques based on a layered manufacturing strategy represent an effective approach for the control at the microscale over the internal architecture as well as the external shape and size of tridimensional (3D)polymeric porous constructs for biomedical applications[22]. The combination of the unique properties of hydrogels and Additive Manufacturing (AM) principles offers a powerful tool for the development of 3D porous structures with a variety of potential applications, such as tissue engineering scaffolds and cell encapsulation carriers[21]. This study contributes to this growing area of research byemploying an AM techniqueinvolving the computer-controlled deposition of a mixture of a polycation (CS) and a polyanion (γ-PGA)to form a microstructured polyelectrolyte complex (mPEC) hydrogel with a 3D interconnected porous architecture.

Hydrogels microstructuring

3D CS or CS/γ-PGAporous hydrogels were successfully fabricated by either freezedrying or CAWS (Figure 1). Freeze-dried hydrogels were obtained by processing CS solutionsormixtures containing both CS and γ-PGAin two different ratios (80:20 and 70:30 CS/γ-PGA weight ratio). SEM analysis showed that the freeze-dried hydrogels were characterized by an interconnected porous structure on both the external surface and in the cross-section with a pore size ranging from 50 to 200 μm (Figure 1a).Freeze-dried CS/γ-PGA PEC hydrogels had lower pore size compared to freeze-dried CS hydrogels,corroborating the results by Tsao *et al*. who reported on a decrease in pore dimension by increasing the degree of CS/γ-PGA complex formation [18].

As shown in Figure 1b, porous hydrogels with a microstructured internal architecture (mCS 100 and mPEC hydrogels) were successfully fabricated by applying the optimized CAWS parameters to process solutions containing CS or a mixture CS/γ-PGA in a 80:20 weight ratio. When processing polymeric solutions containing higher γ-PGA percentages, it was not possible to obtain a continuous extruded filament deposited with a controlled pattern.

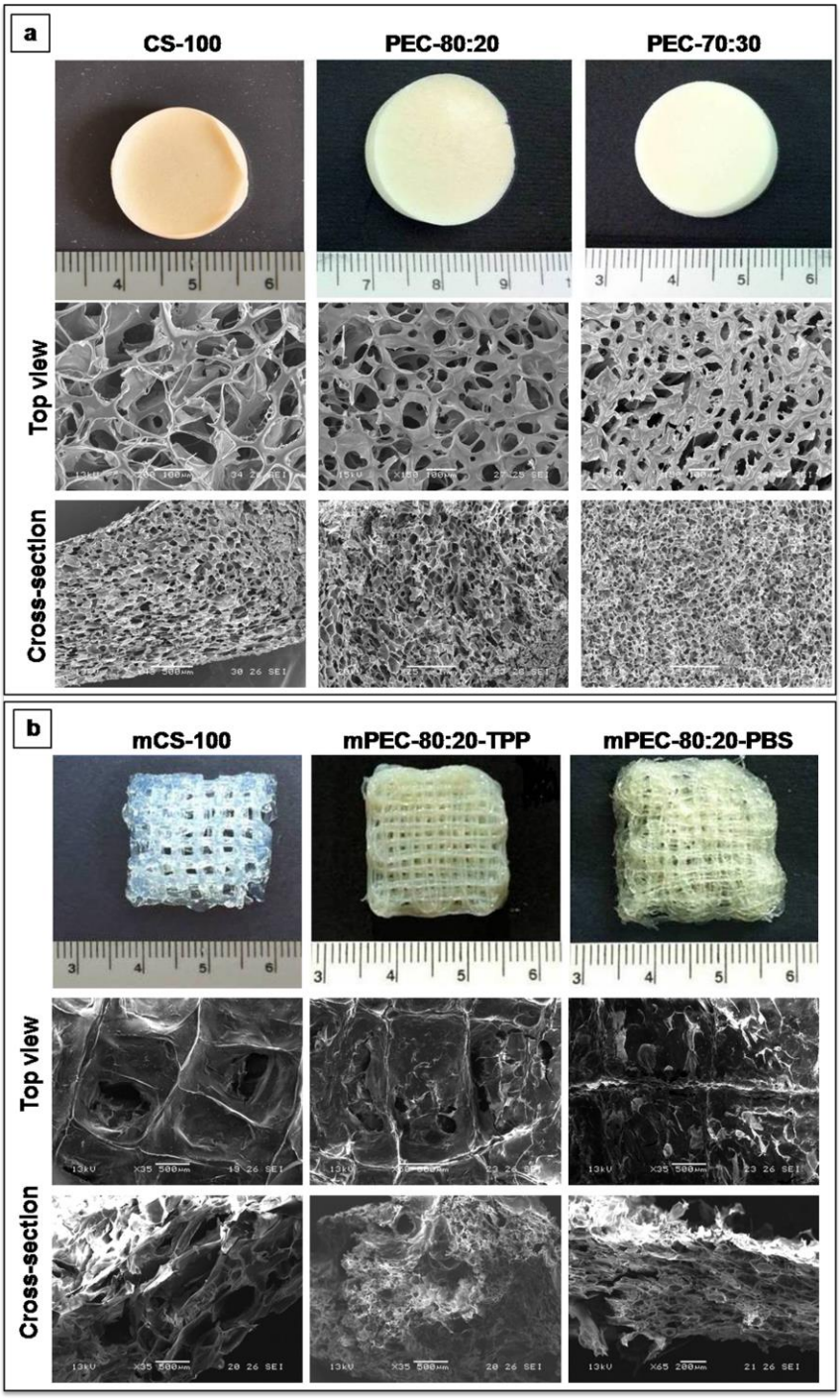

Figure 1. Photographs and SEM micrographs (top view and cross-section) of hydrogels

by (a) freeze drying and (b) CAWS. The layered manufacturing process allowed fabricating 3D porous hydrogels by extruding a CS/γ-PGA mixture.

The fibrous structure of mCS 100 and mPEChydrogels was not clearly visible in SEM micrographs taken from dried samples, even if a porous morphology was still evident, particularly in the samples cross-section.However, the microstructured hydrogels recovered their original geometry and size as well as the aligned fiber architecture upon incubation in aqueous medium. A more defined aligned fiber structure of mPEC hydrogels in comparison to mCS-100 hydrogels was evident from macroscopic observation of wet samples. In addition, the post processing treatment had a marked influence on fibrous morphology. In fact, TPP-treated hydrogels had a more defined fibrous structure with a higher fiber alignment degree in comparison to PBS-treated hydrogels. This effect can be related to an increased crosslinking degree of the mPEC structure. Indeed, TPP is a multivalent ion widely investigated as CS ionic crosslinker for the development of nanoparticles, beads, fibers or 3D scaffolds[10, 30].In acidic medium, the protonated amine groups of chitosan backbone can interact with anionic TPP through electrostatic attraction leading to the formation of a gel[33]. This gelation mechanism was also exploited for fibers wet spinning due to the simultaneous cross-linking and coagulation of chitosan extruded as solution in a TPP containing bath[34, 35].

In comparison with CS/γ-PGA PEC hydrogels developed during previous studies for application as wound dressing and tissue engineering scaffolds [16-19], the developed

mPEC hydrogels present a more controlled porous structure with larger pore size that could be exploited in cell culture experiments for deeper and more uniform cell penetration as well as for enhanced cell nutrients and byproducts mass transfer.

FT-IR spectroscopy analysis

FT-IR spectra of CS and γ-PGA raw, freeze-dried PEC and mPEC hydrogels areshown in Figure 2.

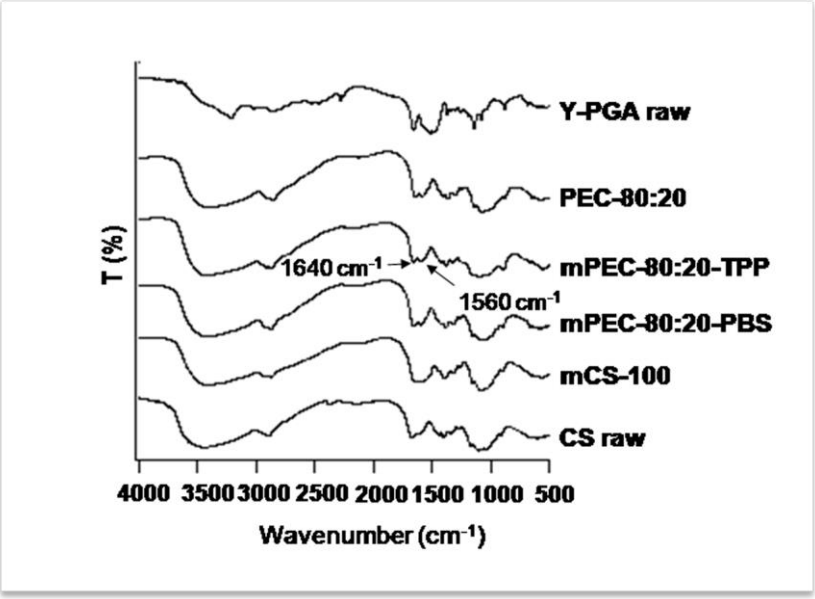

Figure 2. FT-IR spectra of raw polymers, freeze-dried hydrogels and microstructured hydrogels. The shifting of the peak of the (-COOH) groups to 1640 cm-1 and the formation of a new peak at 1560 cm-1 due to bending of the protonated amino groups indicated the formation of an electrostatic complex between CS and γ-PGA.

On analyzing the spectrum of CS, a characteristic broad band at 3431 cm^{-1} was observed corresponding to the overlapping of the stretching vibrations of hydroxyl O-H group and amine N-H_2 groups. C-O stretching vibrations of CS appeared at around 1030 cm^{-1}. The absorption bands of amide I and amide II were detected at 1651 and 1606 cm^{-1}. The peaks at around 894 and 1155 cm^{-1} could be assigned to the saccharide structure. The peak observed at 1424 cm^{-1} was attributed to CH symmetrical deformation mode. The characteristic peaks of γ-PGA appeared at 3400 and 1700 cm^{-1}, corresponding to its N-H bending and carboxylic acid group (-COOH) vibrations, respectively [16].

FT-IR analysis of freeze-driedPEC and mPEC hydrogels confirmed the formation of an electrostatic complex between the two polymers by the shifting of the peak of the (-COOH) of γ-PGA to a lower wavelength (at 1640 nm) and the formation of a new peak at 1560 nm likely due to the NH_3 bending of the protonated amino group on CS. These peaks were evident in both TPP- and PBS-treated mPEC hydrogels highlighting that the ionic complexation between CS and γ-PGA is still present after the two different post-processing treatments.

Determination of swelling degree

The swelling properties of the developed freeze-dried PEC and mPEC hydrogels were studied in PBS1X at 37°C. All the analyzed samples showed similar swelling degree (SD) curves characterized by the reaching of a maximum value after 30 min of immersion followed by a plateau that was roughly maintained in the following hours up

to 20 days (Figure 3).

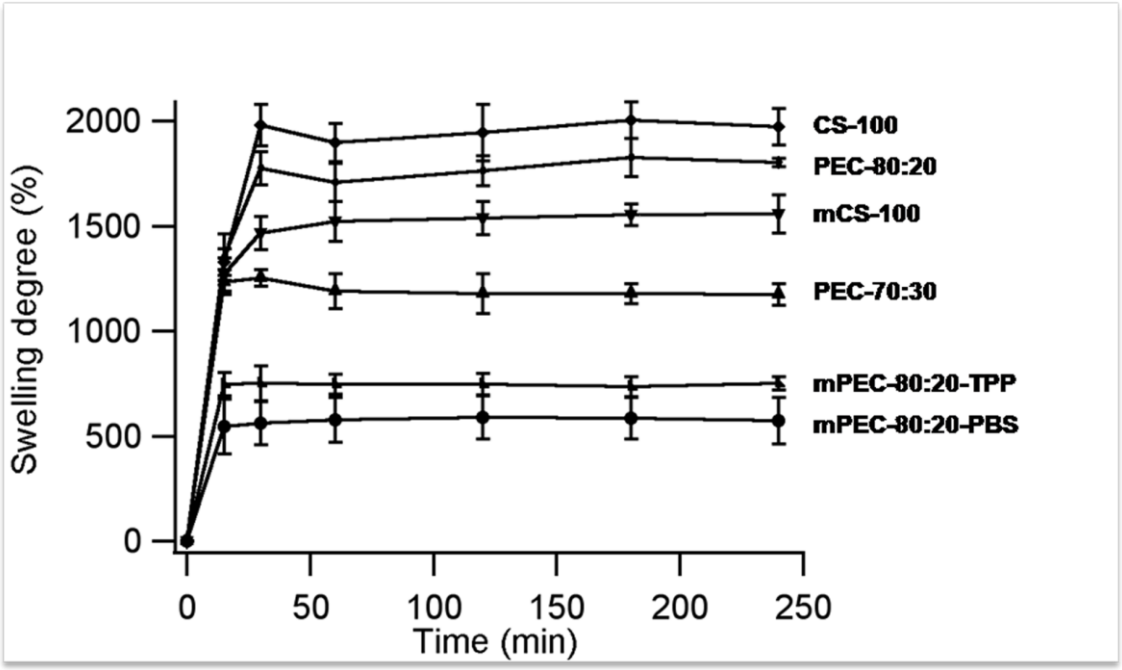

Figure 3. Swelling kinetics of freeze-dried PEC and mPEC hydrogels in PBS 1X at 37 °C. All the samples achieved the equilibrium swelling degree within the first 30 minutes of test.

The equilibrium swelling degree and elasticity of hydrogels depend on various aspects such as the crosslinking degree, charge density and macroporosity of the polymer network [36] as well as the environmental conditions comprising the ionic strength of the surrounding medium. In fact, by increasing the ionic strength, PEC charged groups are shielded by counterions and, as consequence, the hydrogel displays a lower swelling capability [37] resulting in a higher stiffness of the swollen structure [38]. Water

absorption/desorption through an interconnected porous hydrogel structure occurs by convection processes resulting in faster response compared to non-porous hydrogels where mass transfer is governed by diffusion. The swelling equilibrium of CS/γ-PGA PEC hydrogels is determined by the balance of two primary forces: the elastic response of the network and the net osmotic pressure within the network resulting from the mobile counterions surrounding the fixed charge groups [39]. Plain CS hydrogels (CS-100, mCS-100) exhibited higher SD in comparison to the corresponding PEC hydrogels (freeze-dried PEC and mPEC hydrogels). This is in accordance with results from other studies showing that the SD decreased as the degree of complex formation increased, due to the occurring crosslinking effect between CS and γ-PGA [39, 40]. In addition, mPEC hydrogels exhibited overall a lower SD than freeze-dried PEC hydrogels likely due to the different porosity of the 3D constructs.

Thermal analysis

The thermal properties of the developed microstructured hydrogels were investigated in comparison to unprocessed raw polymers and porous hydrogels by freeze drying. Figure 4 provides thermogravimetric (TG) and derivative thermogravimetric (DTG) curves of raw polymers and a physical mixture between raw polymers powders (Figure 4a), freeze-driedPEC and CS 100 hydrogels (Figure 4b), mPEC and mCS-100 hydrogels(Figures 4c).

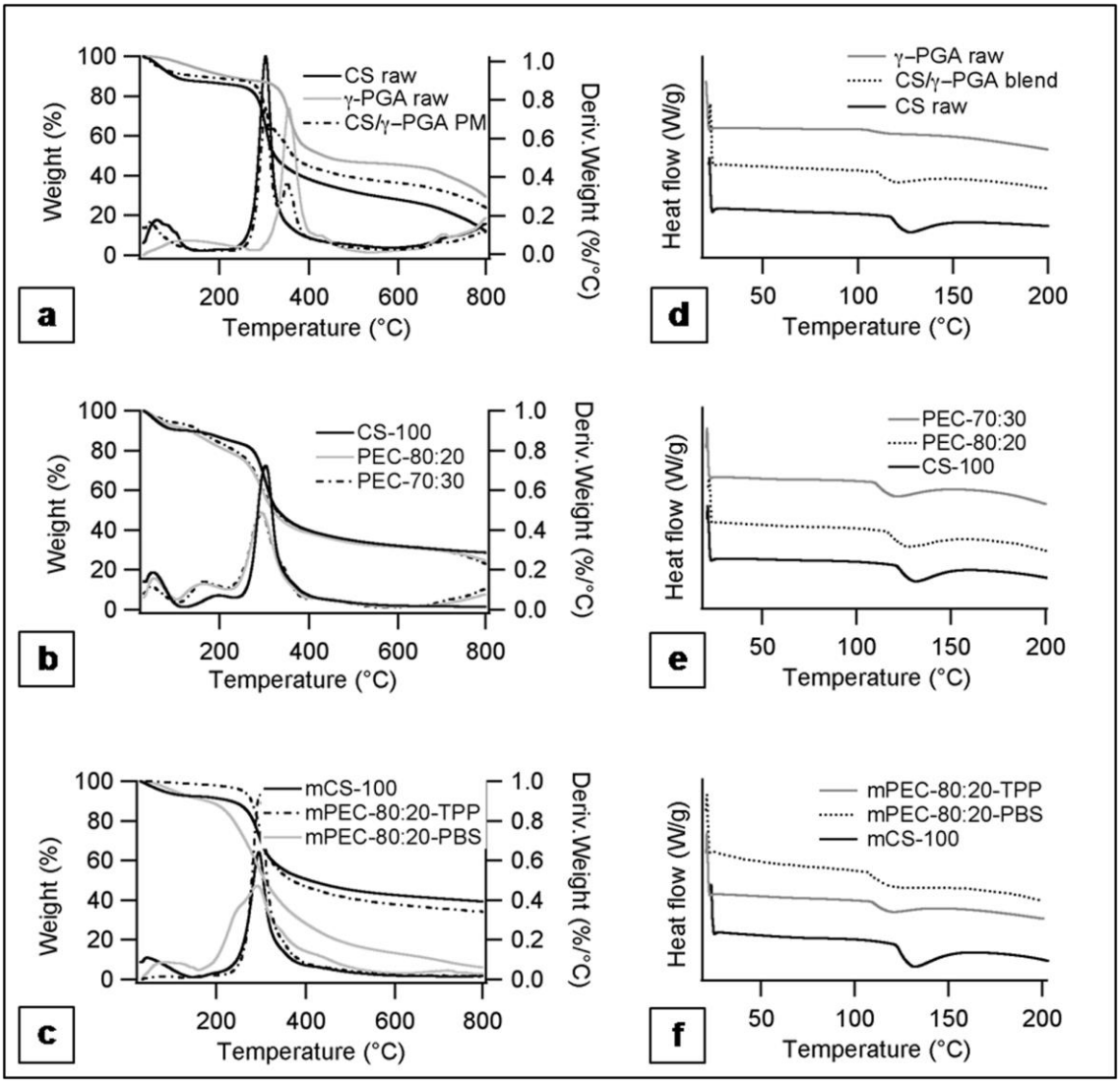

Figure 4. Representative TG and DTG curves of (a) raw polymers (CS raw and γ-PGA raw) and a physical mixture between raw polymers powders (CS/γ-PGA PM); (b) CS-100 and PEC hydrogels by freeze drying; (c) mCS-100 and mPEC hydrogels. mPEC-80:20-TPP hydrogels showed enhanced stability due to the combined TPP and γ-PGA crosslinking. Representative DSC thermograms of (d) raw polymers (CS raw and γ-

PGA raw) and a blend between raw polymers by solvent casting (CS/γ-PGA blend); (e) CS-100 and PEC hydrogels by freeze drying; (e) mCS-100 and mPEC hydrogels. A single Tg at an intermediate value between those of the pure components suggested a good miscibility between CS and γ-PGA.

The DTG curves of all analyzed samples were characterized by a first thermal event in the range 25-140°Ccorresponding to aweight loss of approximately 15% due to the evaporation of absorbed water loosely bound to the polymers [41, 42]. Raw CS exhibited a thermal decomposition peak at around 300 °C that could be attributed to a complex process including dehydration of the saccharide rings, depolymerization and decomposition of the acetylated and deacetylated units of the polymer [17, 41, 42]. Raw γ-PGA analysis showed a decomposition peak at around 350 °C in accordance with a previous study reporting on thermal characterization of different γ-polyglutamate salts, including the sodium salt form[43]. The analysis of the physical mixture between the two raw polymers (CS/γ-PGA weight ratio of 80:20) showed two decomposition peaks roughly corresponding to those of the pure components (Figure 4a). Freeze-driedCS-100 and PEC hydrogels analysis revealed a further degradation stage starting at a lower temperature in comparison with decomposition peaks of raw polymers and polymers physical mixture (Figure 4b). This could be attributed to the more strongly linked structural water as suggested by previous studies on freeze-dried chitosan-based

hydrogels [44, 45]. Moreover, freeze-dried PEC hydrogels were characterized by a lower thermal stability compared to plain CS hydrogels, suggesting that the electrostatic interaction with γ-PGA could alter the crystalline structure of CS, especially through the reduction of hydrogen bonding density[42]. TPP-treated mPEC hydrogels showed the highest temperature corresponding to the main thermal degradation peak, indicating that the combined TPP and γ-PGA crosslinking confer to the structure enhanced thermal stability (Figure 4c).

In order to study the miscibility of CS and γ-PGA, a comparative DSC analysis was carried out on raw polymers and CS/γ-PGA blend films (Figure 4d), freeze-driedCS-100 and PEC hydrogels (Figure 4e), mCS-100 and mPEC hydrogels(Figure 4f). The T_g values, taken at the inflection points in the second cycle thermograms, are summarized in Table 2.

Table 2. Glass Transition Temperature (T_g) of the analyzed samples. Data are reported as mean value ± standard deviation.

Sample	**Glass Transition Temperature (T_g) (°C)**
CS raw	117.6 ± 1.1
γ-PGA raw	106.4 ± 0.9
CS/γ-PGA blend	111.3 ± 1.6

CS-100	122.6 ± 1.8
PEC-80:20	116.3 ± 2.1
PEC-70:30	111.5 ± 1.7
mCS-100	122.2 ± 1.2
mPEC-80:20-PBS	108.4 ± 1.8
mPEC-80:20-TPP	111.7 ± 1.5

Although DSC analysis has been generally assumed not to be sensitive enough to detect the relaxation temperature of CS and CS-based products [46], a glass transition region was clearly detectable in DSC thermograms. Raw CS had a T_g of 117.6 ± 1.1 °C while raw γ-PGA had a T_g of 106.4 ± 1.1 °C. Both freeze-dried PEC hydrogels and mPEC hydrogels showed a single T_g at an intermediate value between those of the pure components, confirming good miscibility between CS and γ-PGA.

Mechanical characterization

The compressive mechanical properties of the developed hydrogels in the swollen state were evaluated using a uniaxial testing machine (strain rate = 0.5 mm/min and maximum strain = 80%) in PBS 1X at 37°C. The stress-strain curves of the tested samples were characterized by an initial low-strain linear region (0-15% strain range) followed by an increase in the curve slope, and a high-strain linear region with higher

stiffness (Figure 5).

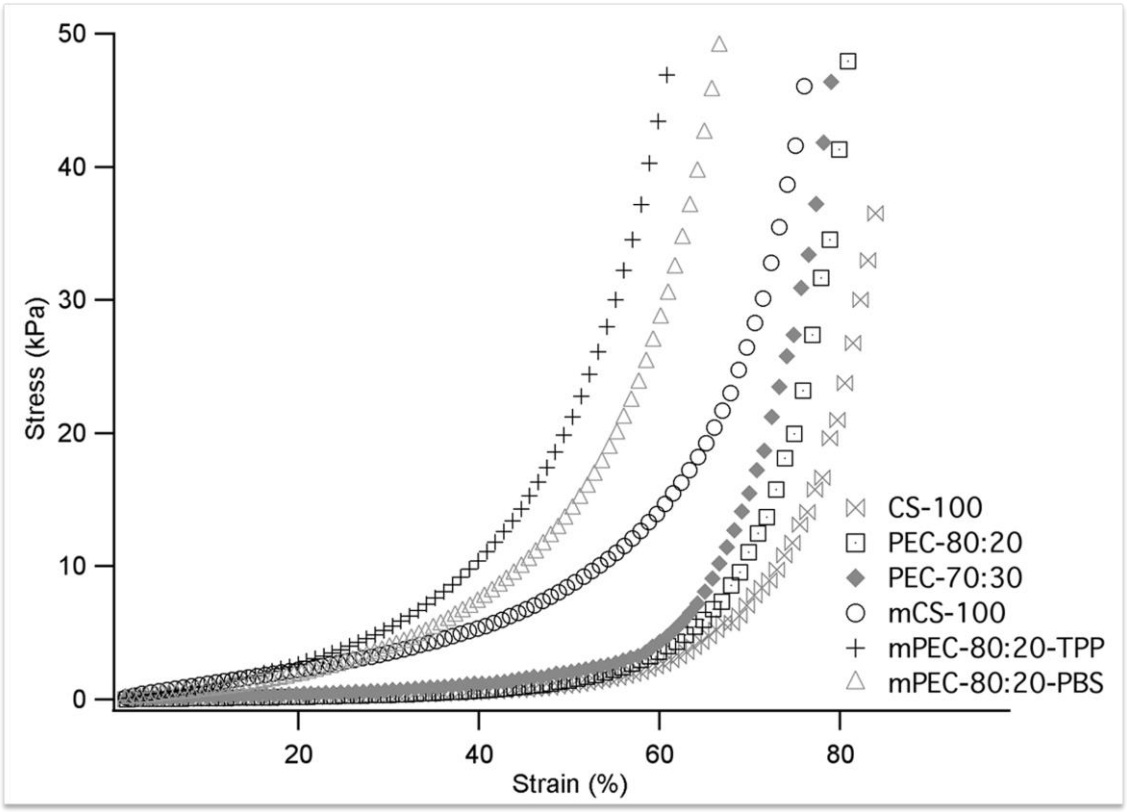

Figure 5. Representative compressive stress-strain curves of the developed freeze-dried and microstructured hydrogels. The combination of the CS/γ-PGA ionic interaction and the defined internal microarchitecture of mPEC hydrogels provided a significant improvement in the hydrogel compressive mechanical properties.

Low-strain and high-strain compressive modulus was defined as the slopes of the two linear portions in the stress-strain curves. Previous studies on microstructured hydrogels suggested that during the low-strain response is a result of the realignment and the

reorganization of the microstructured struts, while the high-strain linear response started at a strain level where struts reorganization becomes difficult, an effect of the close packing of porous structure [47, 48]. The low-strain modulus of the tested hydrogels was in the range 1.5-20 kPa while the high strain modulus was in the range 25-120 kPa (Table 3).

Table 3. Low-strain modulus, high-strain modulus and thickness recovery for the different microstructured hydrogels. Data are reported as mean value ± standard deviation.

Sample	**Low-strain modulus (kPa)**		**High strain-modulus (kPa)**		**Thickness recovery (%)**
	1st Comp. Test	**2nd Comp. Test**	**1st Comp. Test**	**2nd Comp. Test**	
CS-100	1,7 ± 1,4	1,4 ± 0,6	26,5 ± 5,2	7,0±0,7	95,2 ± 4,7
PEC-80:20	2,5 ± 1,5	1,1±0,9	50,8 ± 14,8	9,5±1,7	85,0 ± 4,1
PEC-70:30	2,2 ± 0,6	2,0±1,5	54,8 ± 16,7	11,0±1,1	89,1 ± 6,4
mCS-100	9,5 ± 4,6	2,3±0,3	99,5 ± 1,3	14,1±1,5	93,7 ± 9,0
mPEC-80:20-PBS	11,3 ± 2,9	3,1±1,3	117,9 ± 9,9	17,3±0,6	87,7 ± 2,9
mPEC-80:20-TPP	16,9 ± 3,8	4,1±0,2	118,6 ± 9,2	18,8±2,5	86,8 ± 5,2

1st Comp. Test: the samples were tested at a constant strain rate of 1 mm/min up to 80% strain (PBS 1X, 37°C)
2nd Comp. Test: the mechanical characterization was repeated on the tested samples after incubation in PBS 1X at 37°C for 2 h.

PEC and mPEC hydrogels showed significant higher low- and high-strain modulus than

the corresponding plain CS hydrogels (CS-100 and mCS-100). These results, in agreement with the findings of Tsao *et al*. [16]indicated that the ionic complex interactions between the two polyelectrolyte polymers influence the mechanical properties. In addition, mPEC hydrogels showed significantly higher stiffness than freeze-dried PEC hydrogels. In particular, mPEC-80:20-TPP hydrogels had the highest low-strain modulus further supporting the hypothesis that at low strains a well defined microstructure significantly affects the hydrogel mechanical response [47]. Taken together, these results showed that the combination of the CS/γ-PGA ionic interaction and the defined internal microarchitecture of mPEC hydrogels provided a significant improvement in the compressive mechanical properties.

In order to study the mechanical recovery properties of the developed hydrogels, the tested samples were incubated in PBS 1X for 2 h. After that, their thickness was measured and the compressive analysis was repeated. As summarized in Table 3, the hydrogels were able to recover up to 85-95% of their original thickness. No significant differences in thickness recovery were observed between freeze-dried PEC and mPEC hydrogels. However, the γ-PGA-containing hydrogels showed a significantly lower thickness recovery than the corresponding CS plain hydrogels. Low- and high-strain moduli of freeze-driedand microstructured samples were subjected to a marked decrease after the first compressive test. The comparative results from the first compressive test on differences between hydrogels with different composition as well as between mPEC

and PEC hydrogels were confirmed on the second compressive test.

Cell viability and cell proliferation

The biocompatibility of all the prepared hydrogels and the influence of the scaffold architecture on cell behavior were assessed in a preliminary investigation on cell viability and proliferationof mouse embryo fibroblasts Balb/3T3 clone A31.

Quantitative evaluation of cell proliferation on all the prepared hydrogels, measured at days 2, 5, 8 and 14, highlighted the presence of viable cells on each typeof constructs, starting from day 2. During the culture period, fibroblasts cultured on microstructured hydrogels expressed significantly higher values of cell proliferation when compared to the ones observed for cells grown onto freeze-dried hydrogels ($p<0.05$) (Figure 6a). Moreover, a statistically significant difference ($p<0.05$) was observed between mCS-100 and mPEC-80:20-TPP, highlighting a higher suitability of the microstructured mPEC to support Balb/3T3 cell proliferation.

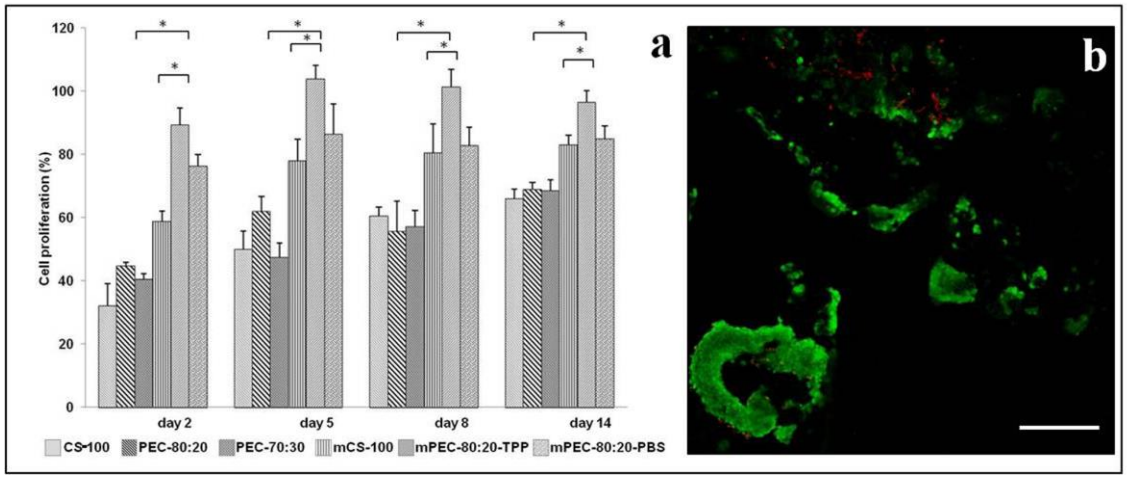

Figure 6. Balb/3T3 clone A31 cell proliferation on freeze-dried and microstructured hydrogels (a) and LIVE/DEAD® staining of Balb/3T3 cultured on mPEC-80:20-TPP (b). * Parameters significantly different ($p<0.05$), scale bar represents 200 □m. mCS-100 and mPEC hydrogels showed significantly higher values of cell proliferation in comparison to freeze-dried hydrogels.

Cell viability was also assessed at day 14 of culture by using LIVE/DEAD® assay. The results were consistent with those obtained by using the alamarBlue®biochemical assay. The CLSM analysis revealed good cell viability with a high live/dead ratio. The visualization of the two fluorescence dyes, with cells mainly stained with green fluorescence, was consistent with a normal cellular adaptation to the hydrogels where only few cells failed to attach to the material and eventually died (red fluorescence). Representative micrograph of LIVE/DEAD® staining of Balb/3T3 clone A31 cells cultured on mPEC-80:20-TPP is reported in Figure 6b.

Cell morphology investigations

SEM analysis was performed at day 14 of culture, both on the top and on the cross-section of all the samples (Figure 7). The SEM investigation revealed that cells colonized differently the various types of the investigated hydrogels. Cells grown on freeze-dried CS-100 and PEC hydrogels displayed spherical morphology with propensity to form clusters (Figures 7a). By contrast, cells grown on microstructured

hydrogels displayed a spread out fusiform shape and features indicative of cell activation, including numerous filopodia and fiber-like protrusions that allowed the anchorage of the cells to the substrate with the formation of a complex multicellular coverage [49] (Figures 7b).

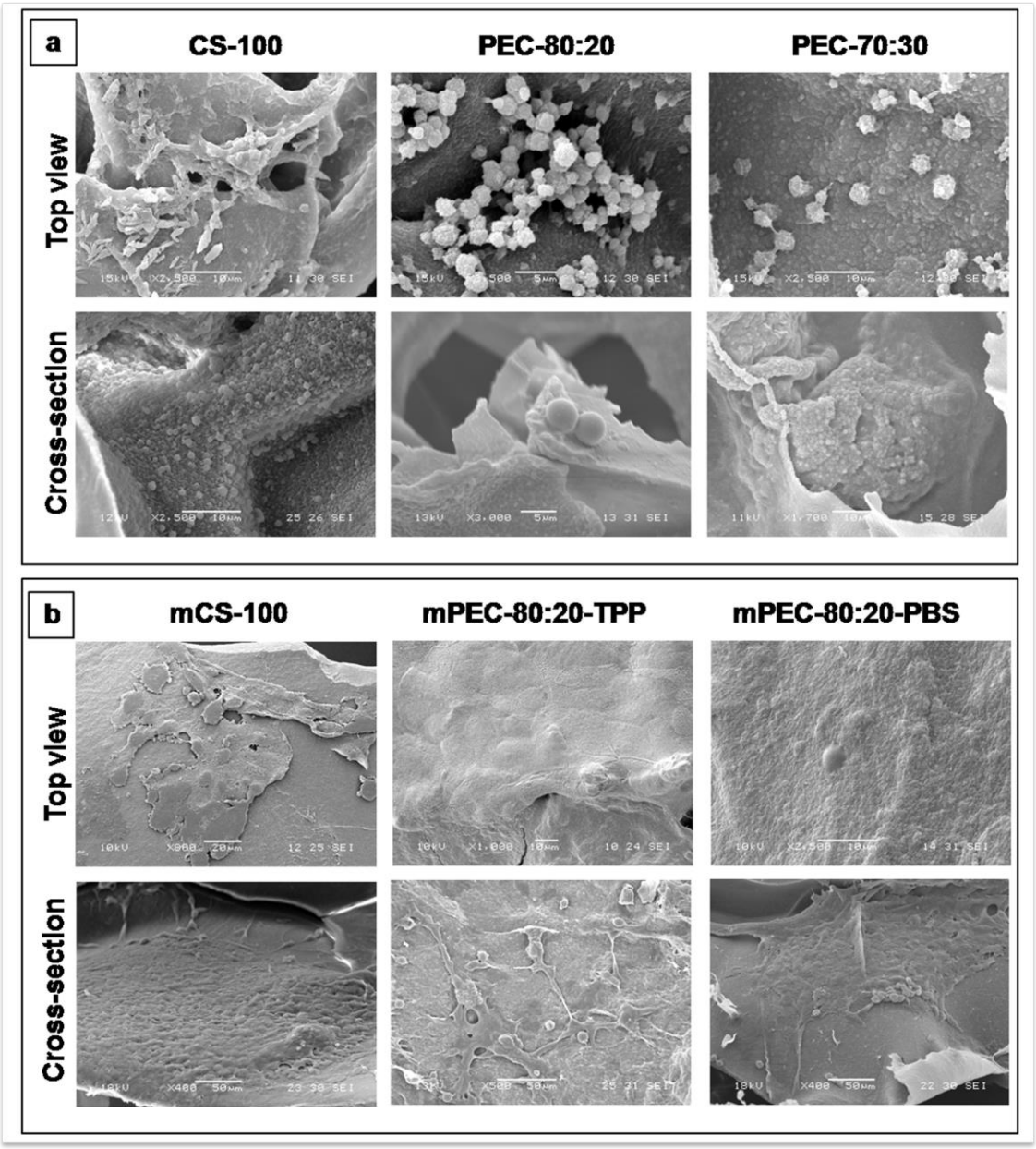

Figure 7. Representative SEM images of Balb/3T3 clone A31 cultured on (a) freeze-dried hydrogels and on (b) microstructured hydrogels (top view and cross-section). Cells grown on freeze-dried hydrogels showed a spherical morphology and were not

uniformly distributed but clustered in colonies, while cells on microstructured hydrogels displayed a spread out and a fusiform shape.

These results were also supported by the CLSM analysis performed at 14 day of culture. Balb/3T3 fibroblasts grown on CS-100 and PEC hydrogels exhibited a spherical morphology typical of a poor cell adhesion (Figure 8a-c), while cells on mCS-100 and mPEC hydrogels displayed a more fusiform shape confirming a better cell adhesion and spreading onto this type of samples (Figure 8d-f). Furthermore micrographs randomly taken throughout cells-cultured microstructured hydrogels showed a high degree of homogeneous cells colonization of the microfibers (Figure 8d-f).

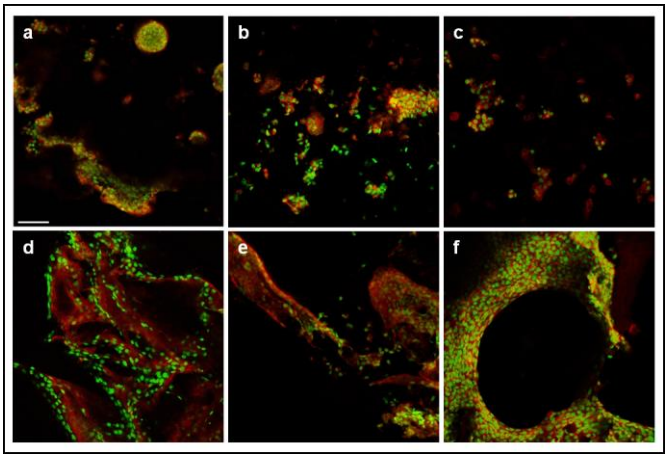

Figure 8. Representative CLSM images of Balb/3T3 clone A31 cultured on CS-100 (a), PEC-80:20 (b), PEC-70:30 (c) mCS-100 (d), mPEC-80:20-TPP (e), mPEC-80:20-PBS

(f) (scale bar represents 100 μm). A high degree of homogeneous cells colonization was observed in microstructured hydrogels.

The performed biological investigations in terms of cell adhesion, proliferation and morphology clearly indicated that the microstructured hydrogel samples promote a better cell response with respect to freeze-dried samples.

These results could be attributed to the different stiffness of the hydrogel matrix that characterizes the various types of the prepared samples, as reported in the section related to the mechanical characterization of the hydrogels. In particular, mPEC hydrogels displayed a higher stiffness in comparison to freeze-dried PEC. As reported by the literature, stiffer substrates generally promote cell spreading, whereas soft substrates induce a more rounded cell shape [50, 51]. Moreover several studies on hydrogel model systems confirmed that matrix stiffness, both initially and over time, had a significant effect on fibroblast activation in *in vitro* cell culture. Fibroblasts responded to increased matrix stiffness by adhering, proliferating and secreting collagen [52].

Conclusions

This research activity has shown that the employed CAWS technique is well suited for microstructuring CS/γ-PGA PEC hydrogels. This approach represents an effective way of combining the advantages of ionic complexation between two biocompatible polyions with those of a hydrogel layered microarchitecture. As demonstrated by the

comparative characterization with freeze dried PEC hydrogels with similar composition, PEC microstructuring has a significant influence on the resulting hydrogel swelling, thermal and mechanical properties. As a consequence, the stiffer microstructured hydrogels obtained by CAWS promoted better *in vitro* cell response in comparison to the freeze dried hydrogels. Considering that hydrogel stiffness has a marked influence on cell adhesion, proliferation and extracellular matrix synthesis, the present study opens new possibilities for the development of novel hydrogel scaffolds for tissue engineering and *in vitro* 3D tissue models. Several studies have reported that even minor variations of hydrogel rigidity have a significant impact on cancer cell survival, growth and phenotypic behavior[53, 54]. The investigation of these mPEC hydrogels for the development of novel *in vitro* cell culture models that could mimic the 3D tissue organization and function of pancreatic ductal adenocarcinoma is the purpose of an ongoing research that will be published in a forthcoming article.

Acknowledgments

Authors are grateful to Dr. Aura Bonaretti for her support in recording SEM images.

Funding

This work was carried out with the financial support by Regione Lombardia (2012) Project “Biomateriali Micro e Nanostrutturati per l’Ingegneria Tissutale derivati da un Polimero Batterico Emergente (PGGABIOMAT)”.

References

1. Morelli A, Puppi D and Chiellini F. Polymers from Renewable Resources. *J Renew Mater*. 2013; 1: 83-112.
2. Puppi D, Chiellini F, Dash M and Chiellini E. Biodegradable Polymers for Biomedical Applications. *Biodegradable Polymers: Processing, Degradation & Applications*. G.P. Felton Ed., Nova Science Publishers, New York, 2011, p. 545-604.
3. Malafaya PB, Silva GA and Reis RL. Natural–origin polymers as carriers and scaffolds for biomolecules and cell delivery in tissue engineering applications. *Adv Drug Deliver Rev*. 2007; 59: 207-33.
4. Peter MG. Chitin and Chitosan from Animal Sources. In: Steinbüchel A, (ed.). *Biopolymers*. Weinheim: WILEY-VCH, 2002, p. 481-574.
5. Di Martino A, Sittinger M and Risbud MV. Chitosan: A versatile biopolymer for orthopaedic tissue-engineering. *Biomaterials*. 2005; 26: 5983-90.
6. Denkbas EB and Ottenbrite RM. Perspectives on: Chitosan Drug Delivery Systems Based on their Geometries. *J Bioact Compat Polym*. 2006; 21: 351-68.
7. Shanmugasundaram N, Ravichandran P, Neelakanta Reddy P, Ramamurty N, Pal S and Panduranga Rao K. Collagen–chitosan polymeric scaffolds for the in vitro culture of human epidermoid carcinoma cells. *Biomaterials*. 2001; 22: 1943-51.
8. Liu IH, Shih-Hsin C and Hsin-Yi L. Chitosan-based hydrogel tissue scaffolds made by 3D plotting promotes osteoblast proliferation and mineralization. *Biomed Mater*. 2015; 10: 035004.
9. Puppi D, Chiellini F, Piras AM and Chiellini E. Polymeric materials for bone and cartilage repair. *Prog Pol Sci*. 2010; 35: 403-40.
10. Dash M, Chiellini F, Ottenbrite RM and Chiellini E. Chitosan—A versatile semi-synthetic polymer in biomedical applications. *Prog Pol Sci*. 2011; 36: 981-1014.
11. Hamman JH. Chitosan Based Polyelectrolyte Complexes as Potential Carrier Materials in Drug Delivery Systems. *Mar Drugs*. 2010; 8: 1305-22.
12. Kunioka M. Biosynthesis and chemical reactions of poly(amino acid)s from microorganisms. *Appl Microbiol Biotechnol*. 1997; 47: 469-75.
13. Bajaj I and Singhal R. Poly (glutamic acid) – An emerging biopolymer of commercial interest. *Bioresource Technol*. 2011; 102: 5551-61.
14. Scoffone V, Dondi D, Biino G, et al. Knockout of pgdS and ggt genes improves γ-PGA yield in B. subtilis. *Biotechnol Bioeng*. 2013; 110: 2006-12.
15. Pacini A, Caricato M, Ferrari S, et al. Poly(γ-glutamic acid) esters with reactive functional groups suitable for orthogonal conjugation strategies. *J Polym Sci Pol Chem*. 2012; 50: 4790-9.
16. Tsao CT, Chang CH, Lin YY, et al. Antibacterial activity and biocompatibility of a chitosan–γ-poly(glutamic acid) polyelectrolyte complex hydrogel. *Carbohydrate Research*. 2010; 345: 1774-80.
17. Tsao CT, Chang CH, Lin YY, Wu MF, Han JL and Hsieh KH. Tissue response to chitosan/γ-PGA polyelectrolyte complex using a rat model. *J Bioact Compat Polym*.

2011; 26: 191-206.
18. Tsao CT, Chang CH, Lin YY, et al. Evaluation of chitosan/γ-poly(glutamic acid) polyelectrolyte complex for wound dressing materials. *Carbohyd Polym*. 2011; 84: 812-9.
19. Chang H-H, Wang Y-L, Chiang Y-C, et al. A Novel Chitosan-γPGA Polyelectrolyte Complex Hydrogel Promotes Early New Bone Formation in the Alveolar Socket Following Tooth Extraction. *PLoS ONE*. 2014; 9: e92362.
20. Wu H-D, Yang J-C, Tsai T, et al. Development of a chitosan–polyglutamate based injectable polyelectrolyte complex scaffold. *Carbohyd Polym*. 2011; 85: 318-24.
21. Billiet T, Vandenhaute M, Schelfhout J, Van Vlierberghe S and Dubruel P. A review of trends and limitations in hydrogel-rapid prototyping for tissue engineering. *Biomaterials*. 2012; 33: 6020-41.
22. Mota C, Puppi D, Chiellini F and Chiellini E. Additive Manufacturing Techniques for the Production of Tissue Engineered Constructs. *J Tissue Eng Regen Med*. 2015; 9: 174-90.
23. Yan Y, Wang X, Xiong Z, et al. Direct Construction of a Three-dimensional Structure with Cells and Hydrogel. *J Bioact Compat Polym*. 2005; 20: 259-69.
24. Wei X, Xiaohong W, Yongnian Y, et al. Rapid Prototyping Three-Dimensional Cell/Gelatin/Fibrinogen Constructs for Medical Regeneration. *J Bioact Compat Polym*. 2007; 22: 363-77.
25. Blatchley MR and Gerecht S. Acellular implantable and injectable hydrogels for vascular regeneration. *Biomed Mater*. 2015; 10: 034001.
26. Puppi D, Mota C, Gazzarri M, et al. Additive manufacturing of wet-spun polymeric scaffolds for bone tissue engineering. *Biomed Microdevices*. 2012; 14: 1115-21.
27. Mota C, Puppi D, Dinucci D, Gazzarri M and Chiellini F. Additive manufacturing of star poly(ε-caprolactone) wet-spun scaffolds for bone tissue engineering applications. *Journal of Bioactive and Compatible Polymers*. 2013; 28: 320-40.
28. Mota C, Wang S-Y, Puppi D, et al. Additive manufacturing of poly[(R)-3-hydroxybutyrate-co-(R)-3-hydroxyhexanoate] scaffolds for engineered bone development. *J Tissue Eng Regen Med*. 2014: DOI: 10.1002/term.897.
29. Puppi D, Zhang X, Yang L, Chiellini F, Sun X and Chiellini E. Nano/microfibrous polymeric constructs loaded with bioactive agents and designed for tissue engineering applications: A review. *Journal of Biomedical Materials Research Part B: Applied Biomaterials*. 2014; 102: 1562-79.
30. Piras AM, Maisetta G, Sandreschi S, et al. Preparation, physical–chemical and biological characterization of chitosan nanoparticles loaded with lysozyme. *Int J Biol Macromol*. 2014; 67: 124-31.
31. Hsieh C-Y, Tsai S-P, Wang D-M, Chang Y-N and Hsieh H-J. Preparation of γ-

PGA/chitosan composite tissue engineering matrices. *Biomaterials*. 2005; 26: 5617-23.
32. Bellucci D, Cannillo V, Sola A, Chiellini F, Gazzarri M and Migone C. Macroporous Bioglass®-derived scaffolds for bone tissue regeneration. *Ceram Int*. 2011; 37: 1575-85.
33. Lee S-T, Mi F-L, Shen Y-J and Shyu S-S. Equilibrium and kinetic studies of copper(II) ion uptake by chitosan-tripolyphosphate chelating resin. *Polymer*. 2001; 42: 1879-92.
34. Pati F, Adhikari B and Dhara S. Development of chitosan–tripolyphosphate fibers through pH dependent ionotropic gelation. *Carbohyd Res*. 2011; 346: 2582-8.
35. Pati F, Adhikari B and Dhara S. Development of chitosan-tripolyphosphate non-woven fibrous scaffolds for tissue engineering application. *J Mater Sci: Mater Med*. 2012; 23: 1085-96.
36. Okay O. General Properties of Hydrogels. In: Gerlach G and Arndt K-F, (eds.). *Hydrogel Sensors and Actuators*. Springer Berlin Heidelberg, 2010, p. 1-14.
37. Gupta NV and Shivakumar HG. Investigation of Swelling Behavior and Mechanical Properties of a pH-Sensitive Superporous Hydrogel Composite. *Iran J Pharm Res*. 2012; 11: 481-93.
38. Cha C, Jeong JH, Shim J and Kong H. Tuning the dependency between stiffness and permeability of a cell encapsulating hydrogel with hydrophilic pendant chains. *Acta Biomaterialia*. 2011; 7: 3719-28.
39. Kang H-S, Park S-H, Lee Y-G and Son T-I. Polyelectrolyte complex hydrogel composed of chitosan and poly(γ-glutamic acid) for biological application: Preparation, physical properties, and cytocompatibility. *J Appl Polym Sci*. 2007; 103: 386-94.
40. Lin W-C, Yu D-G and Yang M-C. Blood compatibility of novel poly(γ-glutamic acid)/polyvinyl alcohol hydrogels. *Colloids Surf, B*. 2006; 47: 43-9.
41. De Britto D and Campana-Filho SP. Kinetics of the thermal degradation of chitosan. *Thermochim Acta*. 2007; 465: 73-82.
42. Singh J, Dutta PK, Dutta J, Hunt AJ, Macquarrie DJ and Clark JH. Preparation and properties of highly soluble chitosan–l-glutamic acid aerogel derivative. *Carbohyd Polym*. 2009; 76: 188-95.
43. Ho G-H, Ho T-I, Hsieh K-H, et al. γ-Polyglutamic Acid Produced by Bacillus Subtilis (Natto): Structural Characteristics, Chemical Properties and Biological Functionalities. *J Chin Chem Soc*. 2006; 53: 1363-84.
44. Horn MM, Martins VCA and de Guzzi Plepis AM. Interaction of anionic collagen with chitosan: Effect on thermal and morphological characteristics. *Carbohyd Polym*. 2009; 77: 239-43.
45. Fernandes LL, Resende CX, Tavares DS, Soares GA, Castro LO and Granjeiro JM. Cytocompatibility of chitosan and collagen-chitosan scaffolds for tissue engineering. *Polimeros*. 2011; 21: 1-6.
46. Dong Y, Ruan Y, Wang H, Zhao Y and Bi D. Studies on glass transition

temperature of chitosan with four techniques. *J Appl Polym Sci*. 2004; 93: 1553-8.
47. Gauvin R, Chen Y-C, Lee JW, et al. Microfabrication of complex porous tissue engineering scaffolds using 3D projection stereolithography. *Biomaterials*. 2012; 33: 3824-34.
48. Soman P, Tobe BD, Lee J, et al. Three-dimensional scaffolding to investigate neuronal derivatives of human embryonic stem cells. *Biomed Microdevices*. 2012; 14: 829-38.
49. Zhang B, Lalani R, Cheng F, Liu Q and Liu L. Dual-functional electrospun poly(2-hydroxyethyl methacrylate). *J Biomed Mater Res A*. 2011; 99A: 455-66.
50. Sunyer R, Jin AJ, Nossal R and Sackett DL. Fabrication of Hydrogels with Steep Stiffness Gradients for Studying Cell Mechanical Response. *PLoS ONE*. 2012; 7: e46107.
51. Breuls RGM, Jiya TU and Smit TH. Scaffold Stiffness Influences Cell Behavior: Opportunities for Skeletal Tissue Engineering. *Open Orthop J*. 2008; 2: 103-9.
52. Smithmyer ME, Sawicki LA and Kloxin AM. Hydrogel scaffolds as in vitro models to study fibroblast activation in wound healing and disease. *Biomater Sci*. 2014; 2: 634-50.
53. Liang Y, Jeong J, DeVolder RJ, et al. A cell-instructive hydrogel to regulate malignancy of 3D tumor spheroids with matrix rigidity. *Biomaterials*. 2011; 32: 9308-15.
54. Aizawa Y, Owen SC and Shoichet MS. Polymers used to influence cell fate in 3D geometry: New trends. *Prog Pol Sci*. 2012; 37: 645-58.